Volume 14
Number 16
28 April 2022
Pages 5931-6270

Nanoscale

rsc.li/nanoscale

ISSN 2040-3372

ROYAL SOCIETY OF CHEMISTRY

PAPER
Scott G. Mitchell, Rafael Martín-Rapún *et al.*
Polyoxometalate–polypeptide nanoassemblies as peroxidase surrogates with antibiofilm properties

NCNST

Nanoscale

PAPER

View Article Online
View Journal | View Issue

Cite this: *Nanoscale*, 2022, **14**, 5999

Polyoxometalate–polypeptide nanoassemblies as peroxidase surrogates with antibiofilm properties†

Héctor Soria-Carrera, [a,b,c] Elena Atrián-Blasco, [a,b] Jesús M. de la Fuente, [a,b] Scott G. Mitchell *[a,b] and Rafael Martín-Rapún *[a,b,c]

Received 14th December 2021,
Accepted 23rd March 2022

DOI: 10.1039/d1nr08223j

rsc.li/nanoscale

Developing artificial metalloenzymes that possess a superior performance to their natural counterparts is an attractive concept. Polyoxometalates (POMs) are a class of anionic molecular metal–oxides with excellent redox properties and bioactivity. We have recently introduced "POMlymers" – covalently conjugated POM–peptide hybrid materials – where the polypeptide chain is obtained through a ring-opening polymerisation (ROP) of α-amino acid *N*-carboxyanhydrides (NCA) on an inorganic POM scaffold. Attracted by the idea of preparing artificial metalloenzymes, here we report the supramolecular self-assembly of POMlymer hybrids into nanoparticles where an optimal environment for catalysis is created. Our results demonstrate that the self-assembly of covalent POMlymers, enhances the peroxidase-like activity of the parent POM anion whereas, in contrast, the catalytic activity for nanoparticles obtained by ionic self-assembly of the same peptide and POM components practically disappears. Furthermore, POMlymer nanoparticles also present antimicrobial and antibiofilm activity against the skin bacterium *Staphylococcus epidermidis*; whereas, ionic POM–peptide hybrids significantly increase biofilm production and endogenous production of reactive oxygen species. In summary, we present the self-assembly of POMlymer hybrids into nanoparticles and a combination of peroxidase activity and microbiology assays that show that the POM–peptide covalent bond is essential for the stability of the self-assembled nanoparticles and therefore for their catalytic and biological activity.

Introduction

Self-assembly is the ultimate degree of complexity designed by Nature to foster activity development and protein evolution underpins such an idea. It is accepted that enzymes emerged from simpler peptides that eventually started to self-arrange into catalytically active assemblies.[1] Peptide folding can further evolve by sequestering metal ions, that once in the structure could synergistically favour catalysis. For instance, Gazit[2] and co-workers prepared a single amino acid enzyme (phenylalanine) that self-assembles into cross-β-sheet nanotubes in the presence of Zn^{2+} and displays hydrolase-like activity. Likewise, Korendovych[3] reported that Zn^{2+} favours β-sheet formation in heptapeptides containing a metal binder residue (histidine) displaying esterase activity. Peptides capable of binding Zn^{2+} should have been important in primitive metabolism. For instance, Moran *et al.*[4] discovered that Zn^{2+} could carry out hydrolytic reactions. Short peptides prone to fold into β-sheets are likely to form amyloids which display catalytic pockets. In consequence, these structures have been proposed to be primitive enzymes on the early Earth.

Polyoxometalates (POMs) – redox-active molecular metal–oxide anions – are extraordinary building blocks that have been widely employed to promote the self-assembly of small molecules and polymers.[5,6] One unique and applicable property of POMs is their excellent redox properties which means that they can potentially display enzymatic behaviour. For example, the group of Parac-Vogt has developed a set of artificial proteases based on POMs which reach a remarkable degree of selectivity.[7] Meanwhile, Wang and co-workers systematically evaluated POMs as peroxidase surrogates, finding comparable efficiencies as horseradish peroxidase (HRP).[8] Eventually, the combination with biomolecules will lead to hybrid materials with synergistic properties. For instance, Wu reported the co-assembly of $K_5PV_2Mo_{10}O_{40}$ with folic acid in nanospheres that promote 3,3′,5,5′-tetramethylbenzidine (TMB) oxidation.[9] Ma *et al.*, reported the preparation of dipeptide–POM–graphene oxide hybrid materials that display peroxi-

[a]*Instituto de Nanociencia y Materiales de Aragón (INMA), CSIC-Universidad de Zaragoza, c/Pedro Cerbuna 12, 50009 Zaragoza, Spain.*
E-mail: scott.mitchell@csic.es, rmartin@unizar.es
[b]*CIBER de Bioingeniería, Biomateriales y Nanomedicina, Instituto de Salud Carlos III, 28029 Madrid, Spain*
[c]*Departamento de Química Orgánica, Facultad de Ciencias, Universidad de Zaragoza, c/Pedro Cerbuna 12, 50009 Zaragoza, Spain*

†Electronic supplementary information (ESI) available: Comprehensive characterisation and antimicrobial activity data. See DOI: https://doi.org/10.1039/d1nr08223j

dase activity superior to the parent POM (Keggin anion PW_{12}).[10]

Co-assembling POMs with peptides has also been recently explored for a wide range of applications in catalysis[11] or biomedicine.[12a,b] For example, in facially amphipathic peptides the addition of POMs triggers fibre formation through β-sheet folding, enhancing the antimicrobial properties of both individual components.[12b] Covalent linking is an alternative strategy to tune hybrid self-assembly. Cronin,[13,14] Coutsolelos,[15] Lacôte[16,17] and Carraro[18,19] have investigated these structures and how both components influence the folding. Ionic interactions between connected POMs and peptides play a key role in the assembly of such hybrids. Recently, Carraro *et al.*[18] reported the use of an anionic spacer, between the POM and the peptide, to preserve the pristine peptide folding.

Likewise, Nature has incorporated metallic clusters in proteins which display crucial roles in metabolic pathways like photosynthesis[20] (Mn_4CaO_5) or oxidative phosphorylation (Fe–S).[21] POMs are present in some natural proteins as well, for example, the molybdenum storage protein (MoSto), involved in the Mo metabolism in N_2 fixating bacteria, displays two sets of polyoxomolybdate POMs: one ionically linked and the other covalently bonded. Remarkably, the protein scaffold not only allocates the POMs inside the peptide chain but also prevents their hydrolysis.[22]

We are interested in developing new synthetic approaches to combining inorganic POM cores with peptides and have recently reported an innovative "on-POM polymerisation" route to obtain covalent POM–polypeptide hybrids, POMlymers. The well-known bis-amino functionalised Mn-Anderson POM derivative $[MnMo_6O_{18}((OCH_2)_3CNH_2)_2]^{3-}$ acts as an initiator for the ring-opening polymerisation (ROP) of amino acid *N*-carboxyanhydrides (NCAs). The first examples, such as $POMK_{10}$ (Fig. 1), display polypeptides comprising cationic and hydrophobic lateral groups along with the central anionic POM. We envisioned that the folding of the polypeptides present in POMlymers[23] could be used to direct the solution-based self-assembly of nanoscale materials to appropriate environments for catalysis. Furthermore, such studies would mean we could expand on the role of the different components involved in generating the antibacterial activity of the POMlymers as well as in their self-assembly.

In recent years, numerous studies have demonstrated that the self-assembly of antimicrobial peptides (AMPs) can boost their antimicrobial activity and also improve their stability.[24–26] This could be one of the many strategies proposed for the development of new antimicrobial agents, necessary to combat antimicrobial resistance (AMR), which is currently deemed to be one of the most important global health threats and is estimated to cause more than 33 000 deaths annually just in Europe.[27,28] While POMs,[29] POM-hybrids[30–32] and POM–peptide assemblies have been described as tailorable new hybrid materials with antimicrobial activity,[12,23,33,34] their mechanism of action has not been explored in detail and has been related, among others, to induced oxidative stress resulting from the production of reactive oxygen species (ROS). ROS can result in hormesis in bacteria, which is characterised by low-dose stimulation and high-dose inhibition. Consequently, high levels of ROS, either internal or external to the cell, can lead to cell death; whereas low levels can trigger an adaptive response from the bacteria, such as increased proliferation or secretion of enzymes and polysaccharides to facilitate the production of biofilm and biofilm matrix.[35] Therefore, understanding how to control the level of ROS produced by antimicrobial materials will aid the development of new antimicrobial agents.

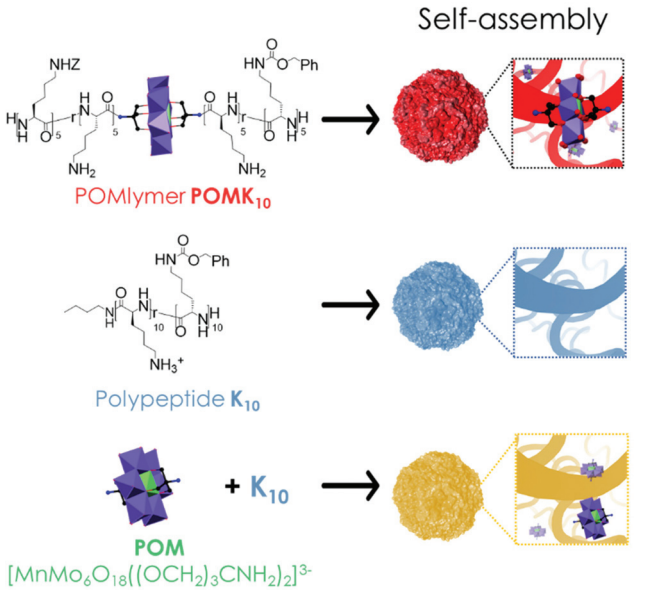

Fig. 1 Structures of POMlymer $POMK_{10}$, polypeptide K_{10} and parent POM, $[Mn^{III}Mo_6O_{18}((OCH_2)_3CNH_2)_2]^{3-}$; and representations of the self-assembled materials under study: POMlymer nanoparticles (red), polypeptide K_{10} assemblies (blue) and ionic K_{10}/POM assemblies (yellow). Z = benzyloxycarbonyl.

Herein we report our systematic study of the self-assembly of POMlymer $POMK_{10}$ – where K_{10} refers to the number of positively charged lysine residues covalently linked to the Anderson–Evans POM – into hybrid nanoparticles and their peroxidase-like properties in the oxidation of TMB. We demonstrate that the covalent hybrid $POMK_{10}$ enhances the catalytic properties of the parent POM $Na_3[Mn^{III}Mo_6O_{18}((OCH_2)_3CNH_2)_2]$, while the ionic assembly of the parent POM and the polypeptide, K_{10}/POM, has a detrimental effect on the catalysis (Fig. 1). Our data suggest that the POM moieties are buried deep inside the self-assembled POMlymer nanoparticle creating a favorable catalytic pocket. Finally, we evaluated the antimicrobial activity of the $POMK_{10}$ nanoparticles against the Gram-positive skin bacterium *Staphylococcus epidermidis* and measured the dose-dependent bacterial response to this redox-active hybrid material by characterising its biofilm production and generation of endogenous ROS.

Results and discussion

Characterisation of POMlymer nanoassemblies

Self-assembly of amphiphilic polymers is a combination of various interactions that results in burying the non-soluble parts of the polymer. In our system, $POMK_{10}$, we have positively charged lysine and hydrophobic lysine – protected as benzyloxycarbonyl (Z) – randomly distributed along the polymer chain (Fig. 1). This combination results in an amphiphilic polymer that can self-assemble in water into nanoparticles of diameter 70.3 ± 18.4 nm, as observed and characterised by dynamic light scattering (DLS) and scanning electron microscopy (SEM) (Fig. 2A & D and Fig. S1 & S2†).

The $POMK_{10}$ nanoparticles display the typical behaviour of polymer-based nanoobjects whose assembly is concentration-dependent (Fig. S3†). The critical aggregation concentration (CAC), which determines the concentration at which the components start to aggregate, could be measured using the hydrophobic solvatochromic probe Nile Red (Fig. S4†) – which also proved the presence of hydrophobic pockets. The corresponding CAC was determined to be 0.34 mg mL^{-1}. Systematic DLS and ζ-potential studies showed that increasing temperature had a detrimental effect on the stability of the $POMK_{10}$ nanoparticles and led to precipitation of the hybrids self-assemblies above 37 °C (Fig. S5†).

Based on previous research[13] we explored how different milieu influence the assembly. We found that increasing the ionic strength (NaCl concentration) led to screening of the polymer charges, which provoked the aggregation of $POMK_{10}$ and low ζ-potentials (Fig. S6†) associated with nanoparticle disassembly. To evaluate the importance of hydrogen bonding in the assembly, we used two well-known chaotropic agents, hexafluoroisopropanol (HFIP) and thiourea (TU), to disrupt the hydrogen-bonding within the assemblies. In general, we observed a variation in size, tending towards larger aggregates and an increase in ζ-potential towards more positive values for both HFIP and TU (Fig. S7 and S8†). We ascribe this effect to the exposure of more lysine groups to the outside since both agents compete for hydrogen bonding. Altogether these studies indicated that ionic interactions must play a crucial role in the $POMK_{10}$ self-assembly process.

$POMK_{10}$ nanoparticles showed a wide range of stability between pH 2 and pH 8.8, as can be seen by the inflection point in the ζ-potential values and the stable hydrodynamic diameter obtained by DLS (Fig. S9†). In addition, circular dichroism (CD) measurements showed a modification in the folding – from an α-helix to a less organised structure – at pH 6 with a subsequent loss of conformation upon further increasing pH (Fig. S10C†).

DLS measurements showed that polypeptide K_{10} and the ionic combination of K_{10} and POM, K_{10}/POM, self-assembled to form 62.6 nm and 60.5 nm nanoparticles respectively, both smaller than those of covalent $POMK_{10}$ (92.3 nm) (Fig. 2A). While $POMK_{10}$ and K_{10} nanoparticles displayed similar ζ-potential (Fig. 2A and S1†), K_{10}/POM displayed a larger ζ-potential. In addition, when we varied the POM-to-K_{10} ratio we observed that ζ-potential linearly increased with POM concentration (Fig. S11B†) despite the anionic POM conferring a large negative charge. Bearing in mind that POMs are also chaotropic agents, we can assume that thiourea and POM behave similarly. In consequence, the POM molecules act to effectively disrupt the peptide folding entering inside the structure which leads to the surface display of previously buried lysine residues. Accordingly, the helical structure of the peptide K_{10} was disrupted upon incorporation of POM molecules into the ionic assemblies K_{10}/POM, as proven with CD spectroscopy measurements (Fig. 2C). Helicity decreased because POM interfered with the hydrogen bonding interactions needed for the α-helix. This unfolding leads to less structured nanoparticles, in which more cationic lysine side chains can emerge to the surface, therefore increasing the ζ-potential value.

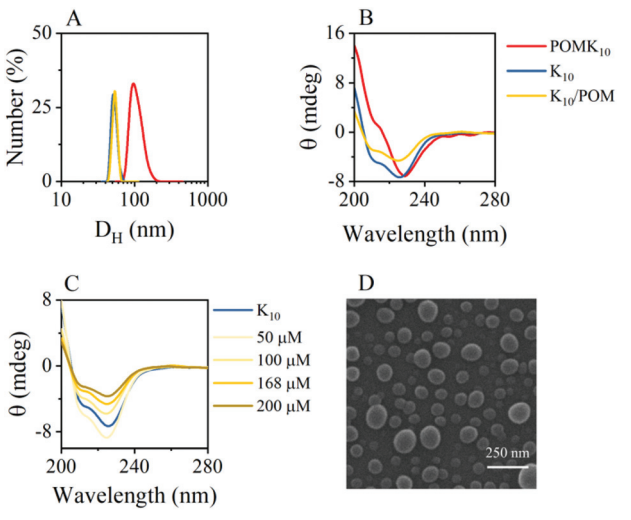

Fig. 2 (A) DLS comparison of the assemblies formed by $POMK_{10}$, polypeptide K_{10}, and the mixture K_{10}/POM (D_H is in log scale, measurements are in water). (B) CD comparison of $POMK_{10}$, K_{10}, K_{10}/POM in water. (C) Variation in the CD of K_{10} upon increasing POM concentration with K_{10} concentration fixed at 1 mg mL^{-1} (*ca.* 192 μM). (D) SEM micrograph of $POMK_{10}$ particles (coated with Pd) possessed a corresponding particle size of 70.3 ± 18.4 nm (N > 200 particles). All experiments were performed at least in duplicate and represented as mean ± SD.

Peroxidase-like activity

$POMK_{10}$ assemblies displayed peroxidase-like activity with the Mn(III) as the redox centre.[36] Steady-state kinetic analysis showed a non-Michaelis–Menten behaviour obtaining a sigmoidal curve in the oxidation of TMB (Fig. 3A and S12–S14†), with partial inhibition at high concentrations. A sigmoidal curve was also observed in the parent POM (Fig. 3A). This behaviour typically appears in allosteric enzymes and can be associated either with multiple catalytic centres or molecular interactions in the catalytic centre. TMB is positively charged in the reaction buffer and so it is likely that it reaches close to the POM, which facilitates the subsequent oxidation. Fitting to the Hill equation we quantified that $POMK_{10}$ had more affinity

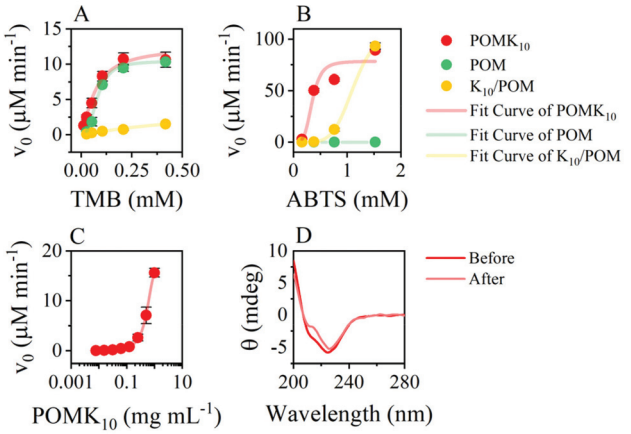

Fig. 3 Steady-state kinetic curves for $POMK_{10}$, parent POM and K_{10}/POM fitted using the Hill equation for (A) TMB and (B) ABTS as substrates. Concentration of POM moiety is 84 μM in all. (C) Initial reaction rates in the oxidation of TMB for different $POMK_{10}$ concentrations (log scale). The solid line represents a Boltzmann fitting whose inset point was calculated[37] as $x_0 - 2dx$ = 0.15 mg mL^{-1}. (D) CD before and after the reaction in a buffered solution (acetate buffer pH 4.6, 10 mM). All experiments were performed at least in duplicate and represented as mean ± SD.

for TMB (K_{half}) than the parent POM, although not statistically significant ($K_{half}^{POMK_{10}} = 69.05 \pm 0.15$ μM and $K_{half}^{POM} = 79.2 \pm 0.3$ μM).

The $POMK_{10}$ nanoparticles significantly reduced in size after the reaction, from 92.3 to 67.1 nm, (Fig. S15†) but retained their secondary structure (Fig. 3D). The reduction in size likely arises to a larger hydrophobic content due to the presence of TMB.

The catalytic activity of $POMK_{10}$ is enhanced when self-assembled. We observed a significant increase in catalytic activity above 0.2 mg mL^{-1} $POMK_{10}$ concentration (Fig. S20†). This concentration is close to the CAC of $POMK_{10}$ in the presence of TMB, which is smaller than for $POMK_{10}$ alone due to the increase of the hydrophobic content (Fig. S21†). These experiments support our hypothesis that the presence of hydrophobic pockets within the assemblies could enhance catalysis. We further verified this concept by disassembling the particles prior to the oxidation reaction of TMB, which led to poor catalytic activity (Fig. S22†).

When we raised the pH, we observed an abrupt decrease in the catalysis above pH 7, which could be attributed to a less charged nanoparticle which could disrupt the catalytic pockets of the assembly (Fig. S16†). We can conclude that the activity of the parent POM was retained in the assembly of the covalent hybrid $POMK_{10}$ while the ionic hybrid K_{10}/POM was considerably less active. We reasoned that the catalytic environment in $POMK_{10}$ nanoparticles is more favourable than in K_{10}/POM.

We explored cooperativity changing the chromogenic probe to 2,2′-azino-bis(3-ethylbenzothiazoline-6-sulfonic acid) (ABTS), which is negatively charged and has a higher reduction potential. In these conditions, ABTS was only oxidised by $POMK_{10}$ (Fig. 3B). However, we observed precipitation of $POMK_{10}$ nanoparticles at high ABTS concentrations, which we ascribe to anionic ABTS acting as crosslinker among positively charged nanoparticles. This was also the case for K_{10}/POM which led to strong scattering and an unreliable apparent increase of initial velocity at higher ABTS concentrations (Fig. 3B and S17–19, [ABTS] = 1.5 mM). Consequently, only $POMK_{10}$ nanoparticles were able to oxidise anionic ABTS, which is an improvement compared to parent POM and K_{10}/POM.

Antibacterial and antibiofilm activity

In our original report on the synthesis of POMlymers,[23] we observed that $POMK_{10}$ could be coated on surfaces to prevent *Bacilus subtilis* biofilm formation. In this study we have researched the antibacterial activity of $POMK_{10}$, as well as the parent POM and the ionic hybrid K_{10}/POM, against the Gram-positive skin bacterium *Staphylococcus epidermidis*. This generally non-pathogenic bacterium forms an important part of human skin microbiota, however it has an important role in nosocomial infections and sepsis in imunocompromised individuals, mainly due to its ability to form biofilms and attach to medical devices.[38] First, we determined the minimum inhibitory concentration (MIC) and minimum bactericidal concentration (MBC) of the different assemblies and compounds, which determine respectively the bacteriostatic and bactericidal activity in solution. Briefly, optical density measurements were used to determine the corresponding MIC values, while a colorimetric resazurin cell viability assay in combination with colony plate-counting were used to verify the MBC values. Self-assembled $POMK_{10}$ possessed a MIC corresponding to 125 μg mL^{-1} (24 μM). The MIC of both polypeptide K_{10} and ionic K_{10}/POM was 62.5 μg mL^{-1}, lower than $POMK_{10}$, while the parent POM had the poorest antibacterial activity with a MIC corresponding to 500 μg mL^{-1} (Table 1). The MBCs of K_{10} and its hybrids were found to be double their corresponding MIC values, rendering all components and assemblies as effective bactericidal agents against the tested model bacterium. Importantly, the antimicrobial activity of the polypeptide and hybrids against Gram-positive bacteria was in the same range as other polypeptidic materials[39–42] and POM–peptide hybrids described in literature.[12,23,33,43]

To better understand the different MIC and MBC values of each material we further studied the early-stage intracellular production of reactive oxygen species (ROS), closely linked to the oxidative stress suffered by the bacteria, in the first hours

Table 1 Minimum inhibitory concentration (MIC) and minimum bactericidal concentration (MBC), in μg mL^{-1}, of the different materials against Gram-positive *S. epidermidis*

	MIC (μg mL^{-1})	MBC (μg mL^{-1})
K_{10}	62.5	125
$POMK_{10}$	125	250
K_{10}/POM	62.5	125
POM	500	>500

of their treatment with the materials. We assessed ROS production using 2′,7′-dichlorodihydrofluorescein diacetate (DCFH-DA) (Fig. 4A). DCFH-DA is a non-fluorescent molecule that is internalised by bacteria and then hydrolysed to produce DCFH. In the event of oxidative stress, DCFH becomes oxidised by H_2O_2 producing fluorescent DCF, thus enabling direct correlation with intracellular production of ROS (Scheme S1†). Therefore, once bacteria had been incubated with DCFH-DA and properly washed to remove any excess of extracellular dye, we added K_{10}, $POMK_{10}$, K_{10}/POM and parent POM at a concentration of 125 μg mL^{-1}, which corresponds to the MIC of $POMK_{10}$ and MBCs of K_{10} and K_{10}/POM (Fig. 4A). The increase of fluorescence intensity, corresponding to the production of DCF and proportional to the ROS formed inside the bacteria, was recorded for at least 90 minutes, and values presented in Fig. 4A were measured 90 minutes after addition of the different treatments, in at least three independent experiments. At first sight, while K_{10} does not promote production of intracellular ROS, the parent POM induces a significant amount of ROS in the first 90 minutes of incubation.

What is more relevant is that production of intracellular ROS is increased in an independent manner to the amount of POM added (Fig. S23†). Treatment with the ionic hybrid K_{10}/POM at 125 μg mL^{-1} leads to a 12-fold increase of ROS, just slightly lower than the parent POM. We reasoned that in the bacterial milieu the ionic assembly loses the POM due to the interactions with the proteins. As a result, the induction of ROS production in K_{10}/POM behaves similarly to the parent POM, and the antibacterial activity the same as K_{10}. In the presence of the covalent hybrid, $POMK_{10}$, the increase in ROS is equal to half that of K_{10}/POM. The origin of the induced intracellular ROS production could be behind an increase in oxidative stress as a defence of the bacteria or as the redox activity of internalized POM. Further studies, which are beyond the scope of this work, will be needed to determine the origin of the increase in intracellular ROS production. Nevertheless, the observed level of ROS production during the first hours of treatment is not lethal to the bacteria, as shown by the corresponding MIC & MBC values obtained for the parent POM. Thus, the antibacterial activity of $POMK_{10}$ is induced by other mechanisms, most likely *via* interaction with the cell membrane, as previously described for cationic AMPs and lysine-based polypeptides.[42,44]

To further assess the effect of ROS and oxidative stress induced by the different materials under study, we conducted the MIC & MBC assays in presence of ascorbic acid (2.5 mM), an important antioxidant and ROS scavenger. ROS quenching by ascorbic acid led to a loss of antibacterial activity of the parent POM and the ionic hybrid, K_{10}/POM, as reflected by the increase of their MBC (Fig. 4C): the MBC of K_{10}/POM doubles from 62.5 μg mL^{-1} to over 125 μg mL^{-1}, and in the case of the parent POM, the MBC value is greater than 500 μg mL^{-1}. This effect has been previously observed in hybrid systems with an important involvement of oxidative stress in the antimicrobial mechanism of action.[35] On the contrary, addition of ascorbic acid seems to have an additive effect on the activity of both K_{10} and $POMK_{10}$ because ascorbic acid greatly reduces *S. epidermidis* growth at concentrations ≥ 5 mM (Fig. S24†). As such we observed that the MBC value of K_{10} decreased by half and there was a visible decrease of bacterial growth for $POMK_{10}$ at 125 μg mL^{-1} (Fig. S25†). These observations from the DCFH-DA and ROS quenching assays seem to indicate that the parent POM has oxidative stress-related activity, although the levels are not enough to produce cell death, whereas the polypeptide and POM–peptide hybrids exert their antibacterial mode of action through an alternative mechanism, or the combination of both.

The morphology of the bacteria inoculated with POM–peptide hybrids and components were studied using SEM to obtain more information about the mechanism of action of the different materials and their possible regulation of biofilm production. K_{10} and $POMK_{10}$ both induced obvious signs of damage to the cell membrane, which collapses in on itself to produce hollow semi-spheres (Fig. 4E). Importantly, *S. epidermidis* treated with K_{10} and $POMK_{10}$ also displayed a greater variability in sizes of bacteria, where significant shrinkage and enlargement of bacteria were both observed (Fig. 4D and E). Furthermore, *S. epidermidis* treated with the parent POM and the ionic hybrid showed an increased production of biofilm matrix, whose components can be seen overlaying and attaching to cell surfaces (yellow arrows in Fig. 4E). Following this observation, we opted to use a crystal violet staining method to quantify the formation of biofilm upon different treatments. Using the crystal violet method, the amount of biofilm produced by *S. epidermidis* was assessed after 72 hours of treatment with the different hybrid nanoparticles or parent POM at their $\frac{1}{2}\times$ MIC values, a concentration which does not kill the bacteria or drastically affect their growth but can have an impact on the production of biofilm (Fig. S26†). The results showed that both K_{10} and $POMK_{10}$ effectively halved the biofilm mass being produced compared with the non-treated bacterial biofilm (Fig. 4B). On the other hand, both the ionic hybrid and the parent POM increased biofilm production, with respect to the non-treated bacteria. First, this could corroborate, as well, the more probable loss of POM from the ionic hybrid in bacterial cell culture broth. Second, the increased biofilm production upon treatment with POM and K_{10}/POM could be related to the increase of the oxidative stress in bacteria treated with these materials: it has been shown that exposure to mild oxidative stress, at least below toxic levels as those presented by POM, could enhance the release of extracellular DNA[45] – an important biofilm matrix component – and bacteria could increase biofilm production as a defence response to oxidative stress.[35] Production of biofilm matrix is also connected to mechanisms of antimicrobial resistance.[46] Therefore, it is important that new antimicrobial materials can inhibit or at least not stimulate the production of biofilm matrix, as well as present an effective antimicrobial mechanism. In this case, our data demonstrate that the $POMK_{10}$ hybrid presents the advantages of both POM and polypeptide in their antimicrobial activities as well as an enhanced inhibi-

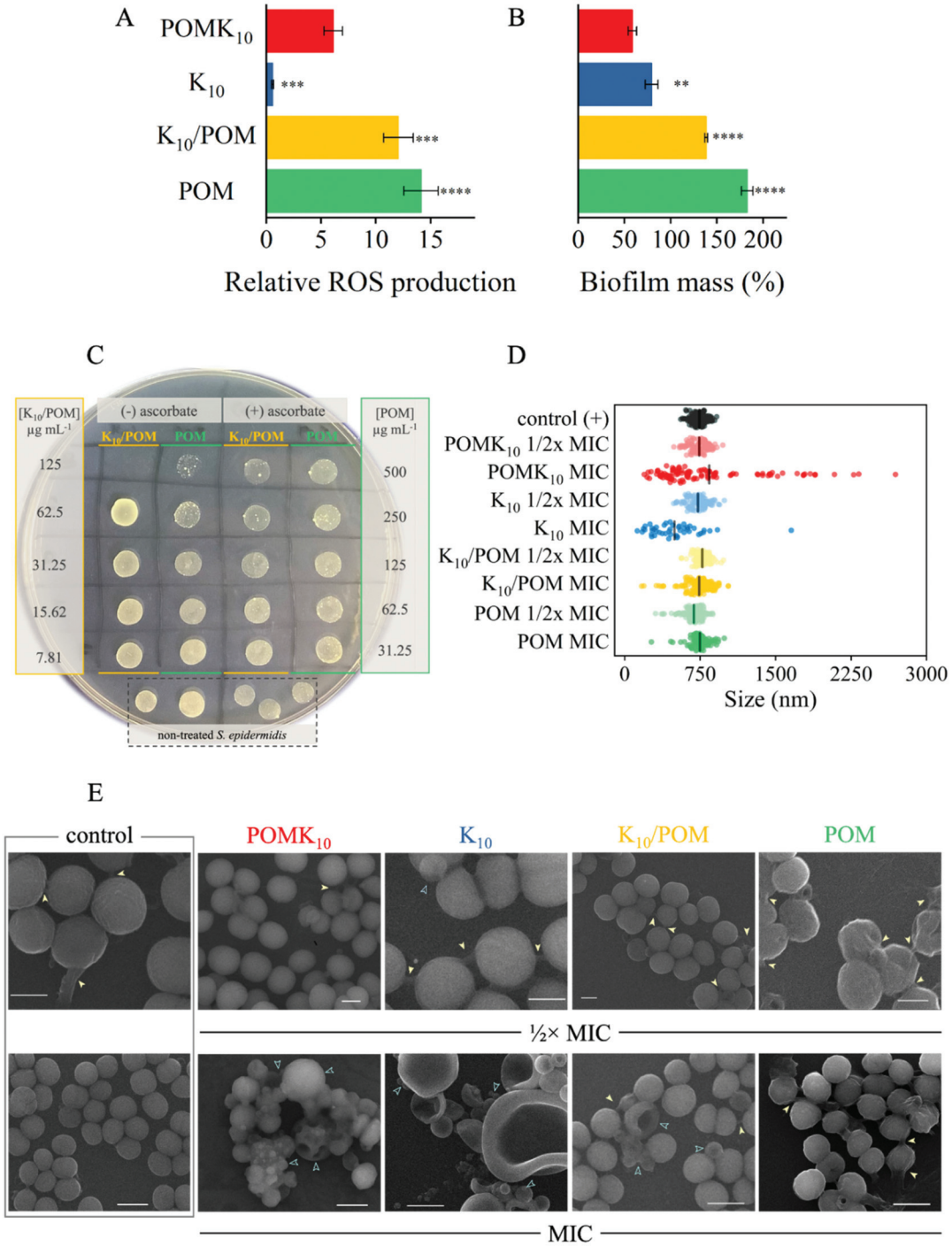

Fig. 4 (A) Intracellular ROS produced by *S. epidermidis* in the presence of 125 μg mL^{-1} of $POMK_{10}$ (red), K_{10} (blue), ionic K_{10}/POM (yellow) and parent POM (green), measured by the fluorescence intensity of produced DCF at λ_{ex} = 488 nm, λ_{em} = 530 nm. The intensity values have been normalized taking as a value of 1 that of the positive control of *S. epidermidis* treated with 1.5 μL of HFIP. (B) Biofilm mass produced by *S. epidermidis* in the presence of 1/2× MIC of $POMK_{10}$ (red), K_{10} (blue), ionic K_{10}/POM (yellow) and parent POM (green) as measured by the absorption of crystal violet. The % values have been normalized, where 0% is the negative control (–), only NB, and 100% is normal *S. epidermidis* growth without any treatment. For both A and B, significance respect to $POMK_{10}$ was evaluated using ANOVA (p < 0.002 ***, p < 0.0002 ***, p < 0.0001 ****). (C) Verification of MBCs of K_{10}/POM and POM on agar plate, with and without addition of 2.5 mM (aq.) ascorbic acid. Values on the left correspond to the concentration of K_{10}/POM and on the right, to the concentration of parent POM. (D) Diameter size distribution of *S. epidermidis* cells without treatment (control) and after treatment with the different compounds, obtained by measurement of at least 100 cells from SEM images. (E) Scanning electron microscopy (SEM) images of *S. epidermidis* without treatment (control) and after incubation with the different compounds at their 1/2× MIC (scale bar = 500 nm) and MIC (scale bar = 1 μm). Yellow arrows indicate biofilm matrix, blue outlined arrows show cell deformation or damage.

tory effect in the production of biofilm. We propose that the covalent POM–peptide hybrids and their self-assembly into spherical nanoparticles represent a promising approach towards the development of antibiofilm materials.

Conclusions

The specific local interactions between components in self-assembled structures expand the possibilities for a material to foster different properties, particularly when compared to the non-assembled individual components. In this study we investigated the role of the covalent connectivity in the aqueous self-assembly of 70 nm diameter POM–polypeptide POMlymer nanoparticles. Our results show that the organisation of the covalent hybrid $POMK_{10}$ into nanoparticles is driven by electrostatic and hydrophobic interactions resulting in the POM being buried in the hydrophobic core. This encapsulation not only preserves the peroxidase-like activity of the parent POM towards the oxidation of TMB, but also permits the oxidation of ABTS – with higher reduction potential. The covalent POM–polypeptide linkage present in the POMlymers is crucial for this improvement, as demonstrated with the negligible catalytic activity of the ionic hybrid K_{10}/POM. Consequently, the assembly of the POMlymer hybrids provides a more robust assembly pathway to preserve the parent POM behaviour and simultaneously expands the substrate scope.

Since living organisms are sensitive to oxidative stress, we evaluated the self-assembled POMlymer against the Gram-positive skin bacterium *S. epidermidis*. We found that the free polypeptide K_{10}, the $POMK_{10}$ - POMlymer - and the ionic K_{10}/POM assemblies all possess antibacterial activity against *S. epidermidis*, whereas the parent POM performs poorly. It is likely that the lower antibacterial activity of the POM can be explained by the production of a non-lethal amount of ROS that acts to stimulate bacterial cell division in order to overcome the external threat. Crucially, while the free polypeptide K_{10} and ionic K_{10}/POM hybrid possessed lower corresponding MIC & MBC values, covalent $POMK_{10}$ POMlymer hybrid significantly reduced biofilm formation, making them appropriate candidates for broad-spectrum antibacterial materials due to the combination of mechanisms of action, which could also help to prevent an antibacterial resistance response.

Author contributions

The idea for the work was conceived by HSC, RMR and SGM. Materials preparation, self-assembly and catalysis studies were performed by HSC and supervised by JMF, SGM, and RMR. Microbiology experiments were carried out by EAB and supervised by SGM. The main hypothesis development and data analysis were undertaken by HSC, EAB, SGM, and RMR. The first draft of the manuscript was written by HSC and EAB. All authors reviewed and edited the final version of the manuscript and approved its submission.

Conflicts of interest

There are no conflicts to declare.

Acknowledgements

This work was funded through the grant PID2019-109333RB-I00 funded by MCIN/AEI/10.13039/501100011033 (Ministerio de Ciencia e Innovación/Agencia Estatal de Investigación, Spain), through project LINKA20270 i-Link+ 2019 funded by CSIC and through Fondo Social de la DGA (grupo DGA E15_20R). HSC is grateful for a predoctoral fellowship FPU2016/02456 funded by Ministerio de Universidades (Spain). E. A. B. and S. G. M. acknowledge funding from the European Union's Horizon 2020 research and innovation program (Marie Skłodowska-Curie grant agreement no. 845427). Authors acknowledge Servicio General de Apoyo a la Investigación-SAI (Universidad de Zaragoza), and the use of instrumentation as well as the technical advice provided by the National Facility ELECMI ICTS, node "Laboratorio de Microscopías Avanzadas" at University of Zaragoza. Particular thanks are given to Gala Simón for advice on SEM analysis, Dr Marta Navarro for support on sample preparation, and Isabel Franco-Castillo for support on microbiology assays.

Notes and references

1 J. Greenwald and R. Riek, *J. Mol. Biol.*, 2012, **421**, 417–426.
2 P. Makam, S. S. R. K. C. Yamijala, K. Tao, L. J. W. Shimon, D. S. Eisenberg, M. R. Sawaya, B. M. Wong and E. Gazit, *Nat. Catal.*, 2019, **2**, 977–985.
3 C. M. Rufo, Y. S. Moroz, O. v. Moroz, J. Stöhr, T. A. Smith, X. Hu, W. F. Degrado and I. v. Korendovych, *Nat. Chem.*, 2014, **6**, 303–309.
4 K. B. Muchowska, S. J. Varma, E. Chevallot-Beroux, L. Lethuillier-Karl, G. Li and J. Moran, *Nat. Ecol. Evol.*, 2017, **1**, 1716–1721.
5 A. v. Anyushin, A. Kondinski and T. N. Parac-Vogt, *Chem. Soc. Rev.*, 2020, **49**, 382–432.
6 P. Gao, Y. Wu and L. Wu, *Soft Matter*, 2016, **12**, 8464–8479.
7 F. de Azambuja, J. Moons and T. N. Parac-Vogt, *Acc. Chem. Res.*, 2021, **54**, 1673–1684.
8 B. Zhang, M. Zhao, Y. Qi, R. Tian, B. B. Carter, H. Zou, C. Zhang and C. Wang, *Sci. Rep.*, 2019, **9**, 1–12.
9 J. Wang, X. Mi, H. Guan, X. Wang and Y. Wu, *Chem. Commun.*, 2011, **47**, 2940–2942.
10 Z. Ma, Y. Qiu, H. Yang, Y. Huang, J. Liu, Y. Lu, C. Zhang and P. Hu, *ACS Appl. Mater. Interfaces*, 2015, **7**, 22036–22045.
11 L. Tong, Z. Wang, C. Xia, Y. Yang, S. Yuan, D. Sun and X. Xin, *J. Phys. Chem. B*, 2017, **121**, 10566–10573.
12 (*a*) J. Xu, X. Li, X. Li, B. Li, L. Wu, W. Li, X. Xie and R. Xue, *Biomacromolecules*, 2017, **18**, 3524–3530; (*b*) J. Li, Z. Chen,

M. Zhou, J. Jing, W. Li, Y. Wang, L. Wu, L. Wang, Y. Wang and M. Lee, *Angew. Chem., Int. Ed.*, 2016, **55**, 2592–2595.
13 J. Luo, B. Zhang, C. Yvon, M. Hutin, S. Gerislioglu, C. Wesdemiotis, L. Cronin and T. Liu, *Eur. J. Inorg. Chem.*, 2019, 380–386.
14 C. Yvon, A. J. Surman, M. Hutin, J. Alex, B. O. Smith, D. L. Long and L. Cronin, *Angew. Chem., Int. Ed.*, 2014, **53**, 3336–3341.
15 E. Nikoloudakis, K. Karikis, M. Laurans, C. Kokotidou, A. Solé-Daura, J. J. Carbó, A. Charisiadis, G. Charalambidis, G. Izzet, A. Mitraki, A. M. Douvas, J. M. Poblet, A. Proust and A. G. Coutsolelos, *Dalton Trans.*, 2018, **47**, 6304–6313.
16 D. Vilona, D. Lachkar, E. Dumont, M. Lelli and E. Lacôte, *Chem. – Eur. J.*, 2017, **23**, 13323–13327.
17 S. Bareyt, S. Piligkos, B. Hasenknopf, P. Gouzerh, E. Lacôte, S. Thorimbert and M. Malacria, *Angew. Chem., Int. Ed.*, 2003, **42**, 3404–3406.
18 V. Tagliavini, C. Honisch, S. Serratì, A. Azzariti, M. Bonchio, P. Ruzza and M. Carraro, *RSC Adv.*, 2021, **11**, 4952–4957.
19 D. Ventura, A. Calderan, C. Honisch, S. Krol, S. Serratì, M. Bonchio, M. Carraro and P. Ruzza, *Pept. Sci.*, 2018, **110**, e24047.
20 B. Zhang and L. Sun, *Dalton Trans.*, 2018, **47**, 14381–14387.
21 M. Fontecave, *Nat. Chem. Biol.*, 2006, **2**, 171–174.
22 B. Kowalewski, J. Poppe, U. Demmer, E. Warkentin, T. Dierks, U. Ermler and K. Schneider, *J. Am. Chem. Soc.*, 2012, **134**, 9768–9774.
23 H. Soria-Carrera, I. Franco-Castillo, P. Romero, S. Martín, J. M. de la Fuente, S. G. Mitchell and R. Martín-Rapún, *Angew. Chem., Int. Ed.*, 2021, **60**, 3449–3453.
24 L. Schnaider, S. Brahmachari, N. W. Schmidt, B. Mensa, S. Shaham-Niv, D. Bychenko, L. Adler-Abramovich, L. J. W. Shimon, S. Kolusheva, W. F. Degrado and E. Gazit, *Nat. Commun.*, 2017, **8**, 1365.
25 X. Tian, F. Sun, X. R. Zhou, S. Z. Luo and L. Chen, *J. Pept. Sci.*, 2015, **21**, 530–539.
26 J. V. Carratalá, N. Serna, A. Villaverde, E. Vázquez and N. Ferrer-Miralles, *Biotechnol. Adv.*, 2020, **44**, 107603.
27 EU Action on Antimicrobial Resistance, **https://ec.europa.eu/health/antimicrobial-resistance/eu-action-on-antimicrobial-resistance_en**.
28 World Health Oganization (WHO), Antimicrobial resistance.
29 A. Bijelic, M. Aureliano and A. Rompel, *Chem. Commun.*, 2018, **54**, 1153–1169.
30 L. de Matteis, S. G. Mitchell and J. M. de la Fuente, *J. Mater. Chem. B*, 2014, **2**, 7114–7117.
31 A. Misra, I. Franco-Castillo, D. P. Müller, C. González, S. Eyssautier-Chuine, A. Ziegler, J. M. de la Fuente, S. G. Mitchell and C. Streb, *Angew. Chem., Int. Ed.*, 2018, 14926–14931.
32 A. L. Kubo, L. Kremer, S. Herrmann, S. G. Mitchell, O. M. Bondarenko, A. Kahru and C. Streb, *ChemPlusChem*, 2017, **82**, 867–871.
33 L. P. Datta, R. Mukherjee, S. Biswas and T. K. Das, *Langmuir*, 2017, **33**, 14195–14208.
34 Y. Zhang, Y. Pi, Y. Hua, J. Xie, C. Wang, K. Guo, Z. Zhao and Y. Yong, *Theranostics*, 2020, **10**, 10031–10045.
35 M. Gambino and F. Cappitelli, *Biofouling*, 2016, **32**, 167–178.
36 J. Luo, Y. Huang, B. Ding, P. Wang, X. Geng, J. Zhang and Y. Wei, *Catalysts*, 2018, **8**, 5–7.
37 J. Aguiar, P. Carpena, J. A. Molina-Bolívar and C. Carnero Ruiz, *J. Colloid Interface Sci.*, 2003, **258**, 116–122.
38 S. Kleinschmidt, F. Huygens, J. Faoagali, I. U. Rathnayake and L. M. Hafner, *Future Microbiol.*, 2015, **10**, 1859–1879.
39 M. Zhou, Y. Qian, J. Xie, W. Zhang, W. Jiang, X. Xiao, S. Chen, C. Dai, Z. Cong, Z. Ji, N. Shao, L. Liu, Y. Wu and R. Liu, *Angew. Chem., Int. Ed.*, 2020, **59**, 6412–6419.
40 H. Sun, Y. Hong, Y. Xi, Y. Zou, J. Gao and J. Du, *Biomacromolecules*, 2018, **19**, 1701–1720.
41 P. Salas-Ambrosio, A. Tronnet, P. Verhaeghe and C. Bonduelle, *Biomacromolecules*, 2021, **22**, 57–75.
42 J. Gao, M. Wang, F. Wang and J. Du, *Biomacromolecules*, 2016, **17**, 2080–2086.
43 C. Zhang, M. Zhao, H. Zou, X. Zhang, R. Sheng, Y. Zhang, B. Zhang, C. Li and Y. Qi, *J. Inorg. Biochem.*, 2020, **212**, 111212.
44 C. D. Fjell, J. A. Hiss, R. E. W. Hancock and G. Schneider, *Nat. Rev. Drug Discovery*, 2012, **11**, 37–51.
45 C. O. Olwal, P. O. Ang'Ienda, D. M. Onyango and D. O. Ochiel, *BMC Microbiol.*, 2018, **18**, 1–13.
46 N. van Gerven, S. E. van der Verren, D. M. Reiter and H. Remaut, *J. Mol. Biol.*, 2018, **430**, 3657–3684.